STUDY ON THE MICROSTRUCTURAL CHANGES IN Zr-2.5Nb DUE TO THE LOCA THERMAL TRANSIENTS

Maria MIHALACHE[1], Vasile RADU[2], Dumitru OHAI[3], Mărgărit PAVELESCU[4]

Analiza accidentelor postulate LOCA în reactoarele PHWR CANDU 6, trebuie să ia în considerare starea de oxidare şi microstructura aliajului Zr-2.5%Nb din care sunt confecţionate tuburile de presiune. În prezentul studiu sunt utilizate tehnici de microscopie optică, electronică de baleiaj (SEM) şi spectrometrie de raze X cu dispersie după enegie (EDS), pentru caracterizarea materialului oxidat în timpul unor cicluri termice LOCA. Probe oxidate izoterm la 700oC, cu grosimi diferite ale oxidului, au fost supuse unor cicluri termice până la 1000oC cu viteze de încălzire/răcire controlate. Modificările microstructurale din stratul de oxid de zirconiu format precum şi ale aliajului de bază sunt corelate cu caracteristicile ciclurilor termice.

Analysis of LOCA postulated in CANDU 6 reactors has to consider the oxidized state and the microstructure of the Zr-2.5%wtNb alloy from which the pressure tubes are made of. During the thermal transients, the microstructural changes both in the oxidized alloy changes int the oxide layer as well as in the material base have been observed by optical microscopy, scanning electron microscopy (SEM) and energy dispersive X-ray spectrometry (EDS). Samples isothermally oxidized at 700oC, with oxide layers of variable thickness, were subjected to various temperature transients up to 1000oC, at different controlled heating/cooling rates. The effects of oxide and alloy microstructural changes were correlated with the characteristics of the thermal transients.

Keywords: oxidation, Zr-2.5%wtNb alloy, pressure tube, CANDU

1. Introduction

Pressurized Heavy Water Reactor (PHWR) uses zirconium base alloys due to their low neutron absorption cross-section, low irradiation creep and high corrosion resistance in operating reactor conditions. Zr-2.5%wtNb alloy, used for pressure tubes from fuel channels, has replaced Zircaloy-2 due to better physical and mechanical properties. The temperature of the coolant fluid from pressure

[1] Senior Researcher III, Institute for Nuclear Research - Pitesti, Nuclear Materials and Corrosion Depart. P.O Box 76, Romania, e-mail: maria.mihalache@nuclear.ro
[2] Senior Researcher III, Institute for Nuclear Research - Pitesti, Nuclear Materials and Corrosion Depart. P.O Box 76, Romania
[3] Senior Researcher III, Institute for Nuclear Research - Pitesti, Nuclear Materials and Corrosion Depart. P.O Box 76, Romania
[4] Prof., member of the Academy of Scientists, Splaiul Independentei street, Bucuresti, Romania

tubes inside varies from 260 ^{o}C (inlet) to 310 ^{o}C (outlet) and its pressure is in 9 to 11 MPa range. Manufacture processes of CANDU pressure tube suppose thermal treatments and a highly anisotropic hexagonal close packed (HCP) microstructure in the as fabricated state [1].

In the LOCA analysis (se explică ce înseamnă acronimul LOCA) the requirement is to maintain the structural integrity of the pressure tube, a third barrier for gas fission products release. During LOCA, if the pressure tube contacts the calandria tube by balooning, a heat transfer between the cooling agent and the moderator at low temperature occurs. The thermal transfer deteriorates if an oxide layer grows on the inner surface of the pressure tube during the thermal transient. This is so because the thermal properties of the oxide are expected to be different than the alloy's, the effect of an oxide layer being the restriction of heat flux transferred to moderator, and a delay of heat release.

One of the major factors affecting the thermo-mechanical behaviour of the pressure tube and the possibility of its failure is the exposure in steam at high temperature [2]. Changes of morphology of zirconium oxide such as layering, spalling, porosity increasing can alter the heat transfer through the pressure tube walls.

The pressure tube may fail due to embrittlement by oxygen, to the formation of a oxide layer and the diffusion of oxygen into the substrate metal. These phenomena can affect the strength and ductility of the pressure tube and lead to failure.

The question that arises is the accurate prediction of the oxide response at thermal stresses produced by thermal transients specific to LOCA. Therefore, the investigation of thermal transients in the oxide layers grown on the pressure tubes, similar to those postulated to happen during an accident conditions can provide a lot of information for the above described problem.

In addition, various methodologies applied for nuclear power plant safety and its management requires a continuous improvement of materials database and models for accurate behavior of fuel channel components during accident scenarios.

In this report we study the oxidized pressure tube microstructure morphology and the embrittlement in thermal transients, covering areas such as: isothermal oxidation, changes of microstructure and behavior of oxidized alloy in thermal transients with different increasing/decreasing rates, elemental composition determination and measurement of oxygen profile in the metal substrate and in the oxide.

The main tools used for evaluations were optical and scanning electron microscopy (SEM) by processing different signals such as secondary electrons, backscattered electrons and also based on energy dispersive X-Ray spectrometry (EDX) and characteristic X-ray spectrum processing.

2. Experimental procedure

2.1 . Starting alloys

The base material used in this study was cold worked Zr-2,5%Nb alloy prevailed from commercial CANDU pressure tubes. As received sample, Pm, corresponds to an α structure containing an alignment of small precipitates (fig 1).

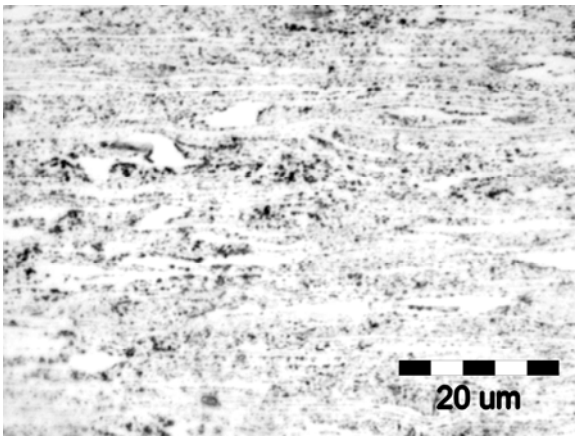

Fig. 1. Optical micrograph showing the microstructure of the Zr-2.5%Nb alloy

Table 1 summarizes the chemical composition and impurities content (% weight) in the investigated alloy. For determining the chemical composition „ARL ADVANT'X Series" fluorescence spectrometer and „UNIQuant" software with a standardless method for spectrum processing have been used.

Table 1.

Elemental composition of investigated Zr2.5%Nb alloy

Zr	Nb	Na	Mg	Si	Fe	Mo
94.51	2.44	2.33	0.32	0.114	0.088	0.063

The accuracy of analysis is evaluated at 0.08 for Nb, 0.07 for Na, 0.015 for Mg and better than 0.01 for the remaining elements. For the laboratory experiments we have used cylindrical samples with 10 mm length and a diameter of 4mm.

2.2. Isotermal oxidation

Four specimens, P1, P2, P4, P7, were heated up to 700^{o}C in a SETARAM SETSYS EVOLUTION 24 thermobalance, and were isothermally oxidized in a flowing steam for different time intervals. The temperature was measured by a Pt-

PtRh10% thermocouple. A Wetsys controlled humidity generator ensured the humidity level control and regulation.

The measurements of weight gains of the samples have been performed in situ. Table 2 presents the parameters and results of the oxidation process for 4 samples.

Table 2

The parameters and results of the oxidation process

Sample	*Initial weight* (g)	*Temperature* (^{0}C)	*Oxidation time* (h)	*Final weight* m_f(g)	*Weight Difference* (mg)	*Weight gain* (mg/dm^2)	*Measured oxide thickness* (μm)	*Oxigen content* (%wt.)
P1	0.74449	700	3	0.74785	3.36	203.33	9	0.451
P2	0.77052	700	6	0.77512	4.60	276.03	10	0.597
P4	0.74200	700	1	0.74376	1.76	106.99	7	0.237
P7	0.72622	700	28	0.73485	8.63	531.57	25	1.188

2.3. Thermal Transients

For simulating LOCA conditions, the samples have been subjected to thermal transients in 25^{o}C – 1000^{o}C temperature range consisting in heating followed by cooling with the same rate in an argon environment. The rates have been: 3, 10, 30, 50, 75^{o}C/min. The thermal treatments and the characteristics of each thermal transient applied to the samples are presented in table 3.

Table 3

Caracteristics of thermal transients

Sample		P0	P1	P2	P7
Transient 1	**Temp range [^{o}C... ^{o}C]**	25-1000	25-1000	25-1000	25-1000
	Cooling rate [^{o}C/min]	10	10	50	30
	Heating Rate [^{o}C/min]	10	10	50	30
Transient 2	**Temp range [^{o}C... ^{o}C]**	-	25-1000	25-1000	25-1000
	Cooling rate [^{o}C/min]	-	30	3	3
	Heating Rate [^{o}C/min]	-	30	3	3
Transient 3	**Temp range [^{o}C... ^{o}C]**	-	25-1000	25-1000	25-1000
	Cooling rate [^{o}C/min]	-	50	10	10
	Heating Rate [^{o}C/min]	-	50	10	10
Transient 4	**Temp range [^{o}C... ^{o}C]**	-	25-1000	25-1000	25-1000
	Cooling rate [^{o}C/min]	-	3	30	50
	Heating Rate [^{o}C/min]	-	3	30	50
Transient 5	**Temp range [^{o}C... ^{o}C]**	-	25-1000	25-1000	25-1000
	Cooling rate [^{o}C/min]	-	75	75	75
	Heating Rate [^{o}C/min]	-	75	75	75

One sample P0 was subjected only to a thermal transient with the rate 10°C/min without any previous oxidation. The SETARAM SETSYS EVOLUTION 24 thermobalance assured the constant rates for heating and cooling and the argon environment. The temperature was measured by means of a Pt-PtRh10% thermocouple.

2.4. Characterization methods

On samples obtained after thermal transients, various phases were observed by optical and scanning electron microscopy. The different microstructures from α, β phases and oxide have been analyzed by means of an energy dispersive X-ray spectrometer (EDS); the fluorescence spectrum was processed using a unfocussed microprobe (3 micrometers) in the points marked on the pictures. The chemical analysis and line profile of elements have been performed by AXS Brucker in SEM using a 30V accelerating voltage.

Samples etched by distilled water 45 cm^3 + HF 10 cm^3 + HNO_3 45 cm^3 were used for putting in evidence the grains shape and size both by optical and scanning electron microscopy.

Unetched samples were used for microprobe analysis. Measured values were corrected by a computer program taking into account the effect of atomic number (Z), absorption (A), and Fluorescence (F) - ZAF method.

3. Results and Discussion

The pressure tubes in current CANDU reactors are made of cold-worked Zr-2.5%wtNb. They are fabricated by hot extrusion, cold drawing and stress relieving at 400°C [3]. Figs. 2 and 3 displays images of grains shape and size in longitudinal and, respectively transverse cross-sections in as received pressure tube, denoted Pm sample. The figures show the dual phase structure of as received pressure tube, with defined texture. The α-phase grains have platelets shape (containing 0.6 - 1% Nb in solution) stacked together and separated by non-equilibrium β phase ~ 20%Nb. Figs. 2 and 3 exhibits a typical α/β structure with uniform and elongated grains in longitudinal cross-section.

The grain sizes are 0.5 μm in radial direction, between 8 and 20 μm in longitudinal direction, and between 1 and 3 μm in transverse direction.

The sample P0, cut from the non-oxidized alloy which was subjected to a thermal transient, changes its microstructure.

Figs. 4 and 5 present images of the shape and size of the grains in sample Po both in longitudinal and transverse cross-sections. Very large β grains can be observed above the temperature of the transition α+β/β. During cooling, inside

the β grains elongated α grains forming Widmanstatten structures have been grown. Other α grains lay on β grain limits, being visible at lower temperatures.

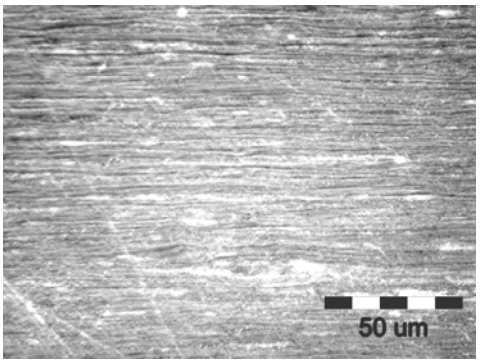

Fig. 2. Optical micrograph of as received sample, Pm (longitudinal cross-section)

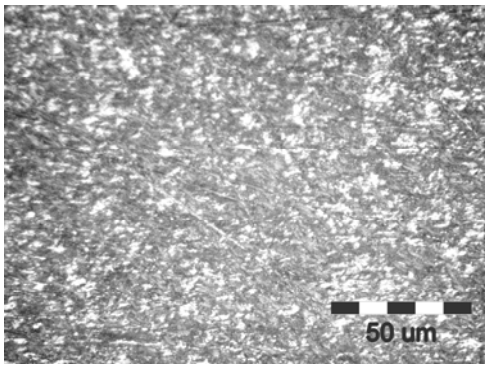

Fig. 3. Optical micrograph of as received sample, Pm (transverse cross-section)

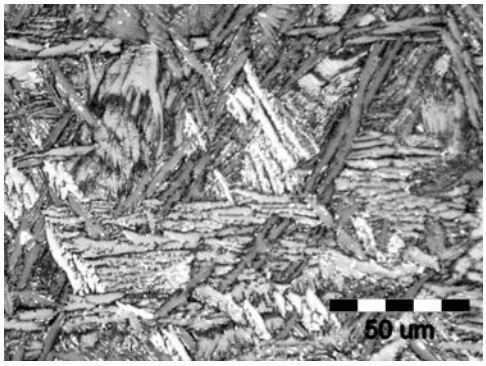

Fig. 4. Optical micrograph of sample Po (longitudinal cross-section)

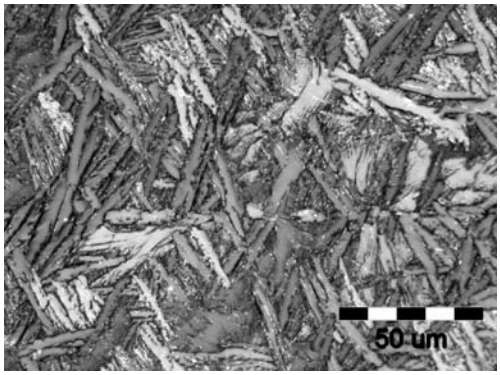

Fig. 5. Optical micrograph of sample Po (transverse cross-section)

On heating microstructural changes occur that affect the mechanical properties[4]. Below 610^{o}C the alloy Zr-2.5%Nb has a monophasic α-phase structure, above 925^{o}C it has a monophasic β-phase structure, while between 610^{o}C and 925^{o}C it has a two-phase structure.

Along with phase changes, recovery of the cold worked structure begins at about 600^{o}C[4], grain growth begins at about 700^{o}C[5], and recrystallization begins at about 800^{o}C. The oxygen content in the alloy changes the (α+β) / β transition temperature [6]. Other changes in the microstructure are possible if an oxide layer is grown on the alloy surface [7]. These microstructural changes complicate the modelling of the mechanical behaviour in thermal transients.

Fig. 6 shows the microstructure at the surface of un-oxidized sample P0, and Fig. 7 at the surface of an oxidized sample P2, after specific thermal transients. Fig. 6 shows that the microstructure is the same at surface as inside the alloy, while if an oxide layer has grown on the surface (as in Fig. 7 on sample P1) then the microstructure beneath the oxide layer presents notable changes.

An oxide layer is found in all oxidized specimens. The oxide can be dense, layered or porous and cracked.

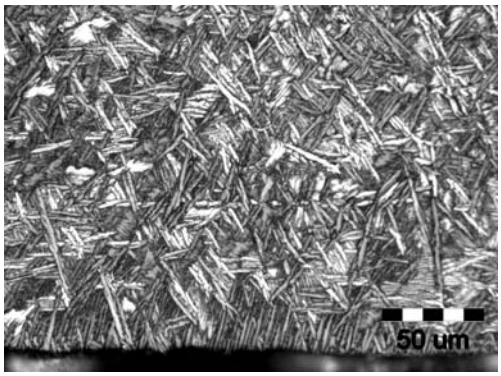

Fig. 6. Optical micrograph at the surface of a unoxidized sample Po.

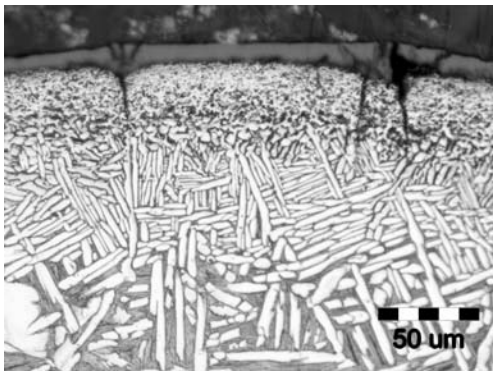

Fig. 7. Optical micrograph at the surface of an oxidized sample P1 after multiple thermal transients

Indeed all Zr-2.5%Nb oxidized samples have a layer with a different microstructure beneath the main oxide layer. This layer was examined by scanning electron microscopy.

The secondary electron (SE) image in Fig. 8a presents a transverse cross-section of the oxidized sample P2. It reveals that just beneath the oxide layer the alloy consists of equiaxed grains with grains sizes increasing with the distance from metal-oxide interface. The SE image of P2 shows a double-layered oxide.

In the BSE image (Fig. 8b) the various microstructural features are differentiated by atomic contrast, namely dark-grey for the oxide (no matter how many layers), light grey for the alloy, and the grain boundaries enriched in niobium that are highlighted in white. The layer with small equiaxed grains (~40 μm in P2 sample) consists in alpha zirconium grains stabilized by the oxide layer or by the oxygen diffused in the alloy during the heating period.

Fig. 9 presents a BSE image of sample P4 in transverse cross-section. Grain boundaries and also an oxide layer consisting in multiple layers are put in evidence. This microstructure was also examined by energy dispersive X-ray spectrometer (EDS); the fluorescence spectrum was processed in the points marked on the picture, in table 3 being presented the results of elemental

composition in each point analyzed. The spectrum was processed by Quantax 400 software with an automatic standardless method (PB/ZAF standardless).

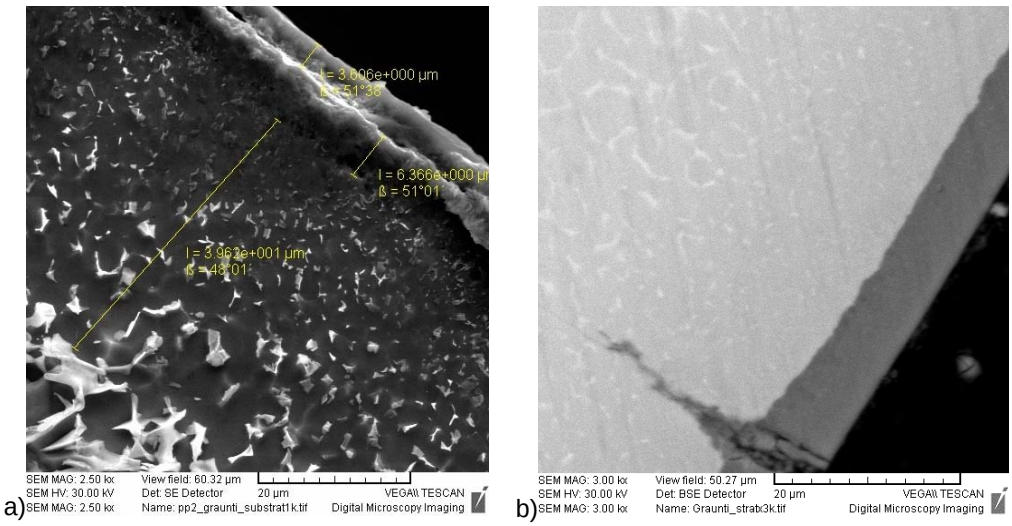

Fig. 8. a) Secondary electron image of P2 sample and (b) back-scattered electron image of P4 sample showing the alloy and oxide microstructures

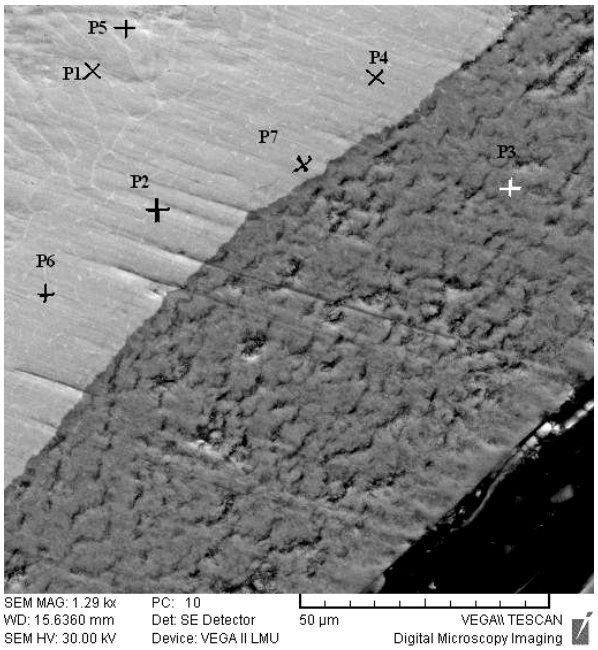

Fig. 9. Atomic contrast back-scattered electron image showing the points for EDS examination

When the oxygen content in zirconium exceeds 26 percent by weight zirconium dioxide forms. From the EDS analysis it seems that point P_3 in Fig. 9 has no niobium content, hence it consists in Zr oxide.

The closest layer beneath the oxide remains in stabilized alpha phase (points P_4, P_7, P_2, P_6), which, in our tests, have value 0 for the oxygen content and ~ 3.5%wt for the niobium content. The EDS results have pointed to a Nb content higher inside the material, above 6%wt. (points P_1, P_5), which was in β –phase at high temperature.

It is clear that less oxygen diffuses into the central region of the tube wall thickness. If the oxygen content of the beta layer remains below certain limits, sufficient ductility is retained to offer resistance to fracture. Consequently, the β layer is the most important layer with respect to pressure tube failures during LOCA.

Table 4

The elemental composition in the points indicated in Fig. 9.

Puncte analizate	Continut Zr [%wt]	Continut O [%wt]	Continut Nb [%wt]
P_1	94	0	6
P_2	96.7	0	3.3
P_3	72.4	27.6	0
P_4	96.5	0	3.5
P_5	93.3	0	6.7
P_6	96.9	0	3.1
P_7	96.8	0	3.2

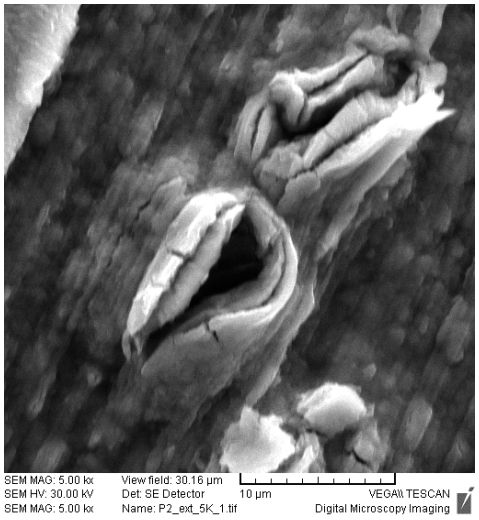

Fig. 10. Cracks în the oxide layer due to thermal stresses(sample P2)

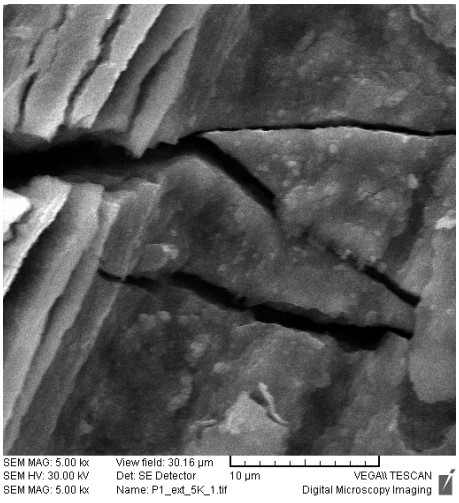

Fig. 11. Cracks în the oxide layer due to thermal stresses(sample P1)

The secondary electron images (Fig.10 and Fig.11), have revealed that the surface oxide films are friable and heavily cracked. They show a lot of cracks in the oxide layer, which can be attributed to thermal stresses due to thermal expansion.

The oxide relaxes by cracking, because it is a brittle ceramic and it is considered to offer no effective resistance to fracture during thermal transients.

Figs. 12 and 13 show a cross-section image of the oxides and alloy microstructures, obtained by optical microscopy.

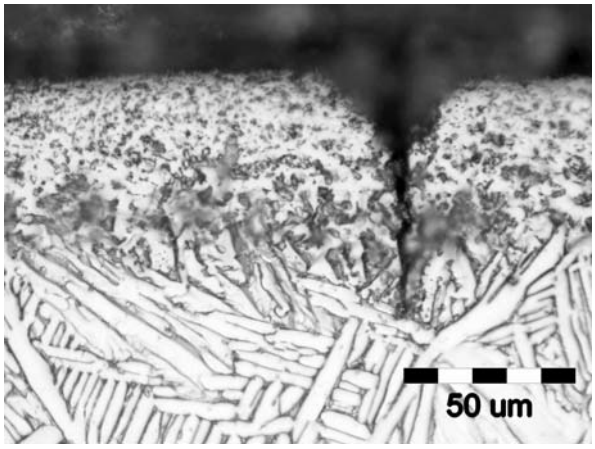

Fig. 12. Optical micrograph of the transverse cross-section of sample P7 showing a crack initiated in the oxide layer, popagated in the Zr stabilised layer and arrested in the Widmanstatten structure

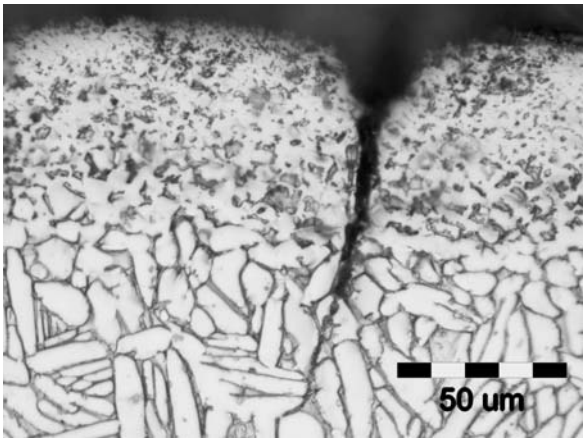

Fig. 13. Optical micrograph of the transverse cross-section of sample P2 showing an intergranular crack propagated in the Widmanstatten structure

The cracks initiated in the oxide have gone through the α–Zirconium layer and arrested in the next layer. Hence one may conclude that the layer immediately under the oxide is also brittle and offer no resistance to fracture by thermal shock.

4. Conclusions

The microstructure analyses carried out on the Zr-2.5%Nb samples that were subjected to thermal transients similar to those from postulated accident as LOCA have put in evidence the following:

a. the oxide layer significantly grows during the thermal transients when the samples are in flowing steam, and in the mean time some microstructural changes of the base alloy occur (grain morphology, phase transforms, etc.);

b. the microstructure changes are characterized by a successive layered structure, regardless of the heat-up/cool down sequences: an oxide layer, a layer of α–Zirconium with equiaxed grains, a Widmanstatten structure (α/β platelets);

c. due to thermal stresses developed during the thermal transients many cracks appear inside the oxide layer, and later on these cracks propagate in the substrate in a transgranular mode being arrested in the Widmanstatten structure;

Therefore, one can conclude that the thermo-mechanical analyses of the CANDU pressure tube behavior have to consider, in a specific way, the degradation of the material properties and the brittle microstructure due to strong oxidation, but also the drastically decreasing of the heat transfer from coolant to the moderator.

REFERENCES

[1] *G. A. Bickel, M. Griffiths* , Manufacturing Variability, Microstructure and Deformation of Zr-2.5%Nb Pressure Tubes, Journal of ASTM International (JAI), **vol. 4**, no. 10, 2007, pp. 35 – 49

[2] *R.N. Singh, K. Kishore, A.K. Singh, T.K. Sinha,* Microstructural Instability and Superplasticity in a Zr-2.5%wtNb Pressure Tube Alloy, Metallurgical and Material Transactions A, Physical Metallurgy and Materials Science, 32(11), 2001, pp. 2827-2840

[3] *K. Kapoor, K. Muralidharan, N. Saratchanran*, Microstructure Evolution and Tensile Properties of Zr-2.5%Nb Pressure Tube Processed from Billets with Different Microstructures, Journal of Material Engineering and Performance, 1999, 8(1), pp. 61-67

[4] *R.G. Fleck, R.A. Holt, V. Perovic and J. Tadros*, Effects of Temperature and Neutron Fluence on Irradiation Growth of Zr-2.5%Nb, Journal of Nuclear Materials, 1988, No. 159, p.75

[5] *M. Uetsura, T. Furuta, A Kawasaki,* Zircaloy-4 Cladding Embrittlement Due to Inner Surface Oxidation under Simulated Loss of Coolant Condition, Journal of Nuclear Science and Technology, 1981, no. 18, pp. 707-717

[6] *R.E. Pawel*, Oxygen Diffusion in Beta Zircaloy During Steam Oxidation, Journal of Nuclear Materials, 1974, no. 50, pp. 247-258

[7] *J.H. Kim, B.K. Choi, J.H. Baek, Y.H. Jeong*, Effects of Oxide and Hydrogen on the Behaviour of Zr-4 Cladding During LOCA, Nuclear Engineering & Design, 2006, no. 236, pp. 2386-2393

[8] *F. Nagase, T. Otowo, H Vetsuka*, Oxidation Kinetics on Low-Sn Zircaloy-4 at the Temperature Range from 773 to 1573, Journal of Nuclear Science and Technology, 2003, no. 40, pp. 213-219.